Space-time discontinuous Galerkin finite element method for inviscid gas dynamics

H. van der Ven [a,*], J.J.W. van der Vegt [b], E.G. Bouwman [b]

[a] Netherlands National Aerospace Laboratory NLR, P.O. Box 90502, 1006 BM Amsterdam, The Netherlands
[b] Department of Applied Mathematics, University of Twente, P.O. Box 217, 7500 AE Enschede, The Netherlands

Abstract

In this paper an overview is given of the space-time discontinuous Galerkin finite element method for the solution of the Euler equations of gas dynamics. This technique is well suited for problems which require moving meshes to deal with changes in the domain boundary. The method is demonstrated with the simulation of the elastic deformation of a wing in subsonic and transonic flow.

Keywords: Discontinuous Galerkin finite element methods; Gas dynamics; Dynamic grid motion; Fluid–structure interaction

1. Introduction

Many problems in fluid mechanics involve flow domains with time-dependent (internal) boundaries. Examples are water waves, fluid structure interaction, multi-fluid flows, and chemically reacting solid–liquid interfaces. The numerical solution of these problems generally requires a moving mesh to accommodate for the changes in the domain boundaries, but this introduces a considerable complexity in the numerical discretization. For instance, it is non-trivial to obtain a conservative discretization for conservation laws on deforming meshes and the frequent remeshing can introduce a substantial interpolation error. In this paper we will discuss a space-time discontinuous Galerkin finite element method which results in a conservative and accurate discretization on moving and deforming meshes.

The main features of the space-time discontinuous Galerkin method are that no distinction is made between the space and time variables in the numerical discretization, and the use of polynomial basis functions which are discontinuous across element faces, both in space and time. This results in a finite element formulation with a very compact stencil, which maintains accuracy on highly non-uniform meshes and can be easily combined with *hp*-mesh adaptation.

The space-time DGFEM technique presently is applied to both parabolic and hyperbolic partial differential equations, but due to space limitations we will only give an outline of the space-time DGFEM for the Euler equations of gas dynamics with an application to the simulation of the elastic deformation of a wing in subsonic and transonic flow. For more details we refer to Van der Vegt and Van der Ven [3,4].

2. Space-time DGFEM for the Euler equations of gas dynamics

We define the Euler equations of inviscid gas dynamics in the space-time domain $\mathcal{E} \subset \mathbb{R}^4$ as:

$$\operatorname{div} \mathcal{F}\big(U(x)\big) = 0, \qquad x \in \mathcal{E}, \tag{1}$$

together with the initial and boundary conditions:

$$U(x) = U_0(x), \qquad x \in \Omega(t_0),$$
$$U(x) = \mathcal{B}(U, U_w), \qquad x \in \mathcal{Q},$$

where $\Omega(t)$ is the flow domain at time t and the space-time domain boundary $\mathcal{Q}$ is defined as: $\mathcal{Q} := \{x \in \partial\mathcal{E} | t_0 < x_0 < T\}$, with t_0 and T the initial and final time of the evolution of the flow domain. The flux tensor $\mathcal{F}\colon \mathbb{R}^5 \to \mathbb{R}^{5\times 4}$ is denoted as:

$$\mathcal{F} = \begin{pmatrix} \rho & \rho u_1 & \rho u_2 & \rho u_3 \\ \rho u_1 & \rho u_1^2 + p & \rho u_1 u_2 & \rho u_1 u_3 \\ \rho u_2 & \rho u_1 u_2 & \rho u_2^2 + p & \rho u_2 u_3 \\ \rho u_3 & \rho u_1 u_3 & \rho u_2 u_3 & \rho u_3^2 + p \\ \rho E & (\rho E + p) u_1 & (\rho E + p) u_2 & (\rho E + p) u_3 \end{pmatrix},$$

* Corresponding author. Tel.: +31 20 511 3773; Fax: +31 20 511 3210; E-mail: venvd@nlr.nl

Computational Fluid and Solid Mechanics 2003
K.J. Bathe (Editor)

with ρ, p, and E the density, pressure, and specific total energy, and u_i the velocity components in the Cartesian coordinate directions x_i, $i \in \{1,2,3\}$ of the velocity vector $u\colon \mathcal{E} \to \mathbb{R}^3$. The first column of $\mathcal{F}$ represents the vector of conservative quantities U, and $U_0\colon \Omega(t_0) \to \mathbb{R}^5$ denotes the initial flow field. The boundary conditions are imposed with the boundary operator $\mathcal{B}\colon \mathbb{R}^5 \times \mathbb{R}^5 \to \mathbb{R}^5$, with $U_w\colon \mathcal{Q} \subset \partial\mathcal{E} \to \mathbb{R}^5$ the prescribed boundary flow field data. The Euler equations are completed with the equation of state for a perfect gas.

The space-time DGFEM is obtained by partitioning the time interval $(0,T)$ into N intervals $I_n = (t_n, t_{n+1})$ and splitting the space-time domain $\mathcal{E} \subset \mathbb{R}^4$ into a finite number of space-time slabs $\mathcal{E} \cap I_n$. In each space-time slab we define a tessellation $\mathcal{T}_h^n$ of space-time elements which are obtained by the linear interpolation of hexahedronal elements at the time levels t_n and t_{n+1}. This allows for deforming elements which can follow (internal) boundaries.

The discontinuous Galerkin finite element discretization uses basis functions in each element which are discontinuous across element faces, both in space and time. The finite element space $V_h^1(\mathcal{T}_h^n)$ is now defined as follows:

$$V_h^1(\mathcal{T}_h^n) := \left\{ U_h \,\middle|\, U_h|_{\mathcal{K}} \in (P^1(\mathcal{K}))^5 \right\},$$

where $P^1(\mathcal{K}) = \operatorname{span}\{\psi_m,\ m = 0,\ldots,4\}$. The basis functions ψ_m are linear in the reference element $\hat{\mathcal{K}} = [-1,1]^4$.

A weak formulation for the space-time DGFEM is obtained by multiplying the Euler equations with the test functions $W_h \in V_h^1(\mathcal{T}_h^n)$ and integrating by parts over the space-time elements $\mathcal{K} \in \mathcal{T}_h^n$. In order to deal with the fact that the test and trial functions are discontinuous at the element boundaries we introduce a numerical flux which is the (approximate) solution of the Riemann problem of gas dynamics. As approximate Riemann solver we use the HLLC flux, because this numerical flux combines excellent shock capturing capabilities with good accuracy and a low computational cost. The numerical flux introduces upwinding into the DGFEM which stabilizes the numerical discretization.

The weak formulation can be formulated as: Find a $U_h \in V_h^1(\mathcal{T}_h^n)$, such that for all $W_h \in V_h^1(\mathcal{T}_h^n)$, the following variational equation is satisfied:

$$-\int_{\mathcal{K}^n} (\operatorname{grad} W_h)^T : \mathcal{F}(U_h)\, d\mathcal{K} + \int_{\partial\mathcal{K}^n} W_h^- \cdot H(U_h^-, U_h^+)\, d\mathcal{Q} + \int_{\mathcal{K}^n} (\operatorname{grad} W_h)^T \cdot \mathfrak{D}(U_h) : \operatorname{grad} U_h \, d\mathcal{K} = 0.$$

The numerical flux at the boundary faces is denoted as $H(U_h^-, U_h^+)$, with $U_h^{\pm}$ the traces of U_h taken from the inside or outside of the element, and contains both the fluxes in space and time. The third contribution is the stabilization operator which is used to prevent numerical oscillations around discontinuities and in regions with insufficient grid resolution.

The weak formulation can be transformed into a system of non-linear equations for the expansion coefficients in each element. These non-linear equations are solved by adding a pseudo-time derivative and integrating in pseudo-time till a sufficiently accurate steady state solution is obtained. The pseudo-time integration is performed with a five stage Runge–Kutta method with optimized coefficients to improve the stability region and damping. In addition, convergence to steady state in pseudo-time is improved using a FAS multigrid technique.

The space-time DGFEM automatically results in a conservative formulation on deforming meshes and is equivalent to an arbitrary Lagrangian Eulerian formulation, which is demonstrated in [3], and provides great flexibility in the mesh deformation since the mesh velocity is independent of the fluid particle velocity.

3. Modelling elastic wing deformation

In order to investigate the capabilities of the space-time DGFEM, as implemented in the flow solver Hexadap, for fluid–structure interaction we simulate the elastic deformation of the AGARD 445.6 wing (Yates et al. [5]; weakened wing number 3). The wing is modelled with a simple beam model, described by the Euler–Bernouilli equations, and allows for bending and torsion due to the external aerodynamic forces. The Euler–Bernouilli equations for the beam deflection and torsion are solved with a standard Galerkin finite element method using cubic Hermite basis functions. For more details on the beam model and the numerical solution, see Reddy [2].

The coupling between the elastic deformation and the flow field is accomplished by computing the aerodynamic forces at a number of wing cross-sections, and adding the gravitational force, after which the beam deflection is calculated with the finite element model. Next, the beam deflection is used to move the wing sections and the modified wing surface is used to compute a new mesh. The present technique only allows for relatively small wing deflections, but is applicable to many aerodynamic problems.

Cross-sectional material properties are estimated from the experimental data, presented in [5], by tuning the bending and torsional stiffness of the beam such that the mode shape frequencies are comparable to the frequencies of the experiment (see Table 1).

The simulations on the AGARD 445.6 wing were conducted for two free stream Mach numbers: 0.45 and 0.96; both at an angle of attack of 2 degrees. The calculations were started from the undeformed shape and continued in time till a steady state was reached. A mesh with 151552 mesh points is used and the results are compared with the finite volume flow solver ENSOLV [1] which is coupled with a fully three-dimensional finite-element model of the

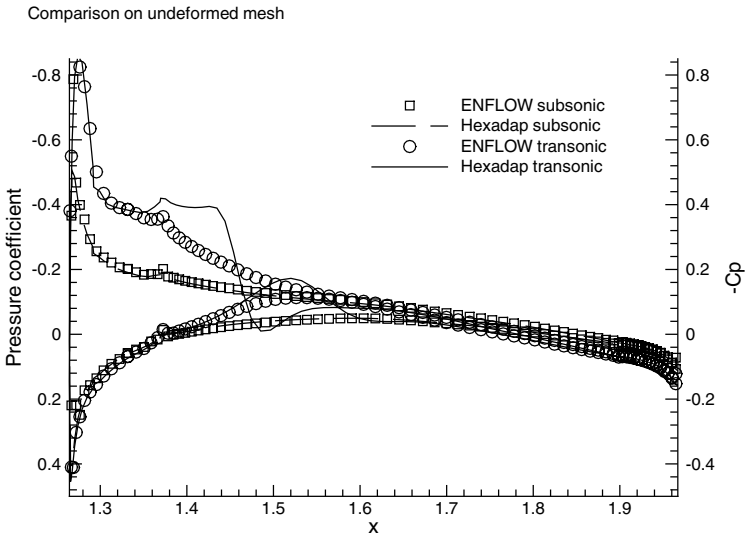

Fig. 1. Comparison of pressure coefficient profiles at 87.5% span for the two flow solvers and Mach numbers.

Table 1
Mode shape frequencies [Hz] of experiment and beam model

Experiment	Beam	Mode shape
9.70	9.708	First bending – torsion
34.89	30.234	Pure torsion
35.00	36.751	First torsion – bending
47.00	56.360	Second bending – torsion
89.50	83.930	Second torsion – bending

AGARD 445.6 wing using NASTRAN. The finite element model of the wing has been tuned to the measured natural frequencies of the wing.

Before comparing the coupled models, the two flow solvers are compared for the two cases on the undeformed wing. In Fig. 1 the pressure coefficient profiles are shown at 87.5% span. The flow solvers agree well for the subsonic case, whereas Hexadap predicts a shock for the transonic case while ENFLOW does not. So we may expect larger deformations for Hexadap in the transonic case because of the resulting increase in lift.

Fig. 2 compares the deflections of the leading and trailing edges for the two methods for the subsonic case. In comparison with the ENSOLV results, the DG solver Hexadap underpredicts the bending displacement, and overpredicts the torsion. The greater (negative) torsion reduces the local angle of attack, and hence the sectional lift, which explains the reduced bending displacement. Since the stand-alone flow solvers agree for the subsonic case, the difference in the results is probably explained by the

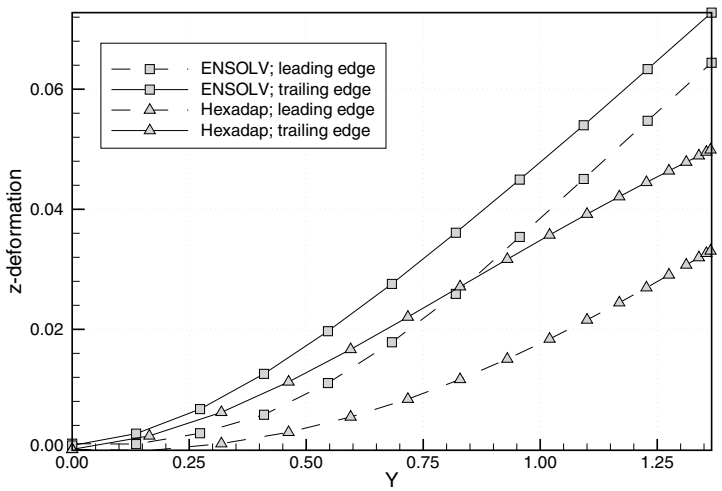

Fig. 2. Comparison of the two methods for Mach = 0.45.

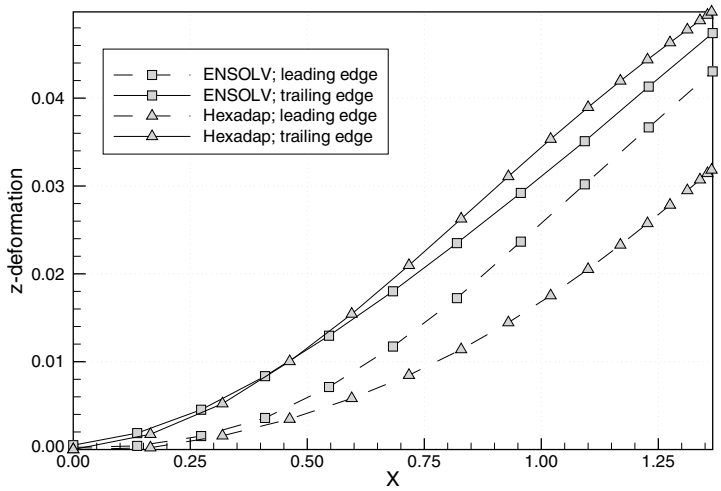

Fig. 3. Comparison of the two methods for Mach = 0.96.

different representation of the structural properties of the wing, leading to larger torsional displacements for the beam model. This is affirmed by the transonic results, which are shown in Fig. 3, and demonstrate the same overprediction of the torsion (and the expected increase in bending displacement due to the increased shock resolution).

4. Conclusions

The space-time DGFEM provides an accurate solution technique to compute subsonic and transonic flows on deforming meshes used to simulate elastic wing deformation. The wing deformation can not be neglected in many cases and future research will concentrate on unsteady problems, in particular helicopter rotors.

Acknowledgements

The research of J.J.W. van der Vegt is supported in part by a research grant from the Netherlands National Aerospace Laboratory, which is gratefully acknowledged. The research of E.G. Bouwman was conducted during a training period at the Netherlands National Aerospace Laboratory. Sincere thanks are due to I.W. Tjatra and B.B. Prananta for supplying the mode shapes of the beam and general discussions on aeroelasticity.

References

[1] Kok JC, Spekreijse SP. Efficient and Accurate Implementation of the k–ω Turbulence Model in the NLR Multi-Block Navier–Stokes System. NLR-TP-2000-144, ECCOMAS 2000, Barcelona, September 2000.

[2] Reddy JN. An Introduction to the Finite Element Method. Wiley, 1993.

[3] Van der Vegt JJW, Van der Ven H. Space-time discontinuous Galerkin finite element method with dynamic grid motion for inviscid compressible flows. I. General formulation. J Comput Phys 2002;182:546–585.

[4] Van der Ven H, Van der Vegt JJW. Space-time discontinuous Galerkin finite element method with dynamic grid motion for inviscid compressible flows. II. Efficient flux quadrature. Comput Meth Appl Mech Engrg 2002;191:4747–4780.

[5] Yates EC, Land NS, Fougher JT, Measured and calculated subsonic and transonic flutter characteristics of a 45° swept-back wing planform in air and freon-12 in the Langley transonic dynamics tunnel. NASA TN D1616, 1989.